Grafting of Polyaniline onto the Surface of 4-Aminobenzoyl-Functionalized Multiwalled Carbon Nanotube and Its Electrochemical Properties

IN-YUP JEON,[1] SANG-WOOK KANG,[1] LOON-SENG TAN,[2] JONG-BEOM BAEK[1]

[1]Interdisciplinary School of Green Energy, Ulsan National Institute of Science and Technology (UNIST), 100, Banyeon, Ulsan 689-897, South Korea

[2]Nanostructured and Biological Materials Branch, Materials and Manufacturing Directorate, U.S. Air Force Research Laboratory, AFRL/RXBN, Wright-Patterson AFB, Ohio 45433

Received 24 February 2010; accepted 16 April 2010
DOI: 10.1002/pola.24091
Published online in Wiley InterScience (www.interscience.wiley.com).

ABSTRACT: Polyaniline (PANi)-grafted multiwalled carbon nanotube (MWNT) composite is prepared by a two-step reaction sequence. MWNT is first functionalized with 4-aminobenzoic acid in polyphosphoric acid/phosphorous pentoxide as a "direct" Friedel-Crafts acylation reaction medium. The resultant 4-aminobenzoyl-functionalized MWNT is then treated with aniline using ammonium persulfate/aqueous hydrochloric acid to promote a chemical oxidative polymerization, leading to PANi-grafted MWNT composite. The resultant composite is characterized by elemental analysis, Fourier-transform infrared spectroscopy, wide-angle X-ray diffraction, scanning electron microscopy, transmission electron microscopy, thermogravimetric analysis, UV–vis absorption spectroscopy, fluorescence spectroscopy, cyclic voltammetry, and electrical conductivity measurement. The thermooxidative stability and electrical conductivity of PANi-grafted MWNT composite are improved compared to those of PANi. Specifically, the electrical conductivity of PANi-grafted MWNT is improved 10–900 times depending upon the level of doping. The capacitance of the composite is also greatly enhanced. © 2010 Wiley Periodicals, Inc. J Polym Sci Part A: Polym Chem 48: 3103–3112, 2010

KEYWORDS: electrochemistry; high-performance polymers; multiwalled carbon nanotube; nanocomposites; polyaniline; polyphosphoric acid

INTRODUCTION Carbon nanotubes (CNTs) have received much interest for their uses in fabricating a new class of advanced materials because of their unique structural, mechanical, and electrical properties.[1] Recent studies have shown that the formation of polymer/CNT composites is considered as a viable approach for an incorporation of CNT into polymer-based devices.[2] Many polymers have been used as matrix materials in polymer/CNT composites for various targeted applications.[3] Among these polymer/CNT composites, many reports have focused on the combination of CNT and conducting polymers including poly(3-ethylenedioxythiophene)/CNT,[4] poly(3-octylthiophene)/CNT,[5] and poly(*p*-phenylene vinylene)/CNT.[6] The resultant polymer/CNT composites have been proposed for a wide range of applications, including an amperometric biosensor for DNA[7] and choline,[8] a sensor for nitrogen oxide,[9] and contact materials in plastic electronic.[10]

Polyaniline (PANi) is unique among the class of conducting polymers, because its doping level can be readily controlled through acid doping–base dedoping processes.[11] In addition, PANi has relatively easy processability, good electrical conductivity, and environmental stability.[3] As a result, PANi has been extensively studied and has the potential to be used as component such as light-emitting or electrochromic devices,[12] sensor,[13] separation membranes,[14] and antistatic coatings.[15] As the hybridization of PANi and CNT could be expected to be more promising materials, many reports on PANi/CNT systems have been reported for optoelectronic and sensor applications.[16] To disperse CNT and thus to provide maximum surface interactions between polymer and CNT interfaces, hitherto, harsh chemical treatments in strong acids such as sulfuric acid, nitric acid or their mixtures, and/or physical treatments such as sonication have been commonly applied.[17] These treatments work well to improve dispersability. Unfortunately, these approaches often result in significant damage to the CNT framework, which involve sidewall opening, breaking, and turning into amorphous carbon.[18] The damage on CNT would definitely diminish their original outstanding properties such as electrical, thermal, and physical properties.[19] In addition to the damage issue, strong interfacial adhesion between polymer and CNT is a prerequisite to efficiently transfer the outstanding properties

Additional Supporting Information may be found in the online version of this article. Correspondence to: J.-B. Baek (E-mail: jbbaek@unist.ac.kr)
Journal of Polymer Science: Part A: Polymer Chemistry, Vol. 48, 3103–3112 (2010) © 2010 Wiley Periodicals, Inc.

Report Documentation Page

Form Approved
OMB No. 0704-0188

Public reporting burden for the collection of information is estimated to average 1 hour per response, including the time for reviewing instructions, searching existing data sources, gathering and maintaining the data needed, and completing and reviewing the collection of information. Send comments regarding this burden estimate or any other aspect of this collection of information, including suggestions for reducing this burden, to Washington Headquarters Services, Directorate for Information Operations and Reports, 1215 Jefferson Davis Highway, Suite 1204, Arlington VA 22202-4302. Respondents should be aware that notwithstanding any other provision of law, no person shall be subject to a penalty for failing to comply with a collection of information if it does not display a currently valid OMB control number.

1. REPORT DATE **2010**	2. REPORT TYPE	3. DATES COVERED **00-00-2010 to 00-00-2010**
4. TITLE AND SUBTITLE **Grafting of Polyaniline onto the Surface of 4-Aminobenzoyl-Functionalized Multiwalled Carbon Nanotube and Its Electrochemical Properties**		5a. CONTRACT NUMBER 5b. GRANT NUMBER 5c. PROGRAM ELEMENT NUMBER
6. AUTHOR(S)		5d. PROJECT NUMBER 5e. TASK NUMBER 5f. WORK UNIT NUMBER
7. PERFORMING ORGANIZATION NAME(S) AND ADDRESS(ES) **Ulsan National Institute of Science and Technology (UNIST),Interdisciplinary School of Green Energy & Inst of Advanced Materials & Devices,100, Banyeon,Ulsan 689-798, South Korea,**		8. PERFORMING ORGANIZATION REPORT NUMBER
9. SPONSORING/MONITORING AGENCY NAME(S) AND ADDRESS(ES)		10. SPONSOR/MONITOR'S ACRONYM(S) 11. SPONSOR/MONITOR'S REPORT NUMBER(S)

12. DISTRIBUTION/AVAILABILITY STATEMENT
Approved for public release; distribution unlimited

13. SUPPLEMENTARY NOTES

14. ABSTRACT
Polyaniline (PANi)-grafted multiwalled carbon nanotube (MWNT) composite is prepared by a two-step reaction sequence. MWNT is first functionalized with 4-aminobenzoic acid in polyphosphoric acid/phosphorous pentoxide as a ??direct?? Friedel-Crafts acylation reaction medium. The resultant 4-aminobenzoyl-functionalized MWNT is then treated with aniline using ammonium persulfate/aqueous hydrochloric acid to promote a chemical oxidative polymerization, leading to PANi-grafted MWNT composite. The resultant composite is characterized by elemental analysis, Fourier-transform infrared spectroscopy, wide-angle X-ray diffraction, scanning electron microscopy, transmission electron microscopy, thermogravimetric analysis, UV?vis absorption spectroscopy, fluorescence spectroscopy, cyclic voltammetry, and electrical conductivity measurement. The thermooxidative stability and electrical conductivity of PANi-grafted MWNT composite are improved compared to those of PANi. Specifically, the electrical conductivity of PANi-grafted MWNT is improved 10? 900 times depending upon the level of doping. The capacitance of the composite is also greatly enhanced.

15. SUBJECT TERMS

16. SECURITY CLASSIFICATION OF:			17. LIMITATION OF ABSTRACT	18. NUMBER OF PAGES	19a. NAME OF RESPONSIBLE PERSON
a. REPORT **unclassified**	b. ABSTRACT **unclassified**	c. THIS PAGE **unclassified**	**Same as Report (SAR)**	**10**	

of CNT to the supporting polymer matrix, and thus maximally enhanced properties from resultant composites can be expected. However, most of previous approaches involve that CNT is physically dispersed in conducting polymer matrices with secondary interaction such as van der Waals attraction. The interaction may not be strong enough for the ultimate transfer of CNT properties. Thus, covalent links between CNT and polymer matrix would be a better option.

As our initial foray into the area of CNT chemistry, the less destructive chemical modification of various carbon nanomaterials via electrophilic substitution reaction in a mild polyphosphoric acid (PPA)/phosphorous pentoxide (P_2O_5) medium has been developed.[20] It is a so-called "direct" Friedel-Crafts acylation reaction, which is advantageous over conventional Friedel-Crafts acylation because most of substituted benzoic acids can be used instead of corrosive and less commercially available benzoyl chlorides. Although there is little or no structural damage to the functionalized CNT (F-CNT) in PPA/P_2O_5 medium, the covalent attachment of organics onto the sidewall of CNT could still disrupt the electronic continuum. Consequently, their surface electrical and thermal conductivities could be somewhat sacrificed. To overcome the problem, the covalent grafting of conducting polymer onto the surface of F-CNT could be a viable approach to minimizing diminution of the electrical conductivity. Considering the ample precedents, we have demonstrated that the grafting of poly(phenylene sulfide) onto the surface of 4-chlorobenzoyl-functionalized MWNT significantly enhances the electrical conductivity of the resultant composite.[21] The hybridization of the ubiquitous conducting polymer PANi and CNT has remained an important challenge.

Herein, we report the preparation of 4-aminobenzoyl-functionalized multiwalled carbon nanotube (AF-MWNT) and grafting of PANi onto the surface of AF-MWNT to afford PANi-grafted MWNT composite (PANi-*g*-MWNT). AF-MWNT with reactive aromatic amine groups, where PANi could be grafted from, was prepared from the reaction between the 4-aminobenzoic acid and MWNT in the mild PPA/P_2O_5 medium. A subsequent chemical oxidation polymerization between aniline as monomer and AF-MWNT was conducted in ammonium persulfate (APS)/1 M aqueous hydrochloric acid (HCl) to yield PANi-*g*-MWNT. The resultant composites showed improved thermal stability, conductivity, and capacitance compared with those of PANI homopolymer.

EXPERIMENTAL

Material

All reagents and solvents were purchased from Aldrich Chemical and Lancaster Synthesis and used as received, unless otherwise specified. MWNT (CVD MWNT 95 with diameter of ~20 nm and length of 10–50 μm) was obtained from Hanhwa Nanotech, Seoul, Korea.

Instrumentation

Infrared (IR) spectra were recorded on Jasco FTIR 480 Plus spectrophotometer. Solid samples were embedded in KBr disks. Elemental analyses (EA) were performed with a CE Instruments EA1110. Thermogravimetric analysis (TGA) was conducted in air atmosphere at a heating rate of 10 °C min^{-1} using Perkin–Elmer TGA 7. The field emission scanning electron microscopy (FE-SEM) used in this work was done using LEO 1530FE and NanoSem 230. The field emission transmission electron microscopy (FE-TEM) was done using a FEI Tecnai G2 F30 S-Twin. The Brunauer-Emmett-Teller (BET) surface area was measured by nitrogen adsorption–desorption isotherms using Micromeritics ASAP 2504N. Wide-angle X-ray diffraction (WAXD) powder patterns were recorded with a Rigaku RU-200 diffractometer using Ni-filtered Cu Kα radiation (40 kV, 100 mA, $\lambda = 0.15418$ nm). UV–vis spectra were obtained on a Perkin–Elmer Lambda 35 UV–vis spectrometer. Stock solutions were prepared by dissolving 10 mg of each sample in l L of *N*-methyl-2-pyrrolidone (NMP). Photoluminescence measurements were performed with a Perkin–Elmer LS 55 Fluorescence spectrometer. The excitation wavelength was that of the UV absorption maximum of each sample. Cyclic voltammetry (CV) experiments were performed with a 1470E Cell Test System (Solartron Analytical, UK). The test electrodes were prepared by dipping glassy carbon sheet into sample solution in NMP and the electrode was dried and used as working electrode. The CV experiment was conducted in 1.0 M aqueous sulfuric acid solution with a scan rate of 10 mV s^{-1} and in the potential of −0.2 and 1.2 V. The three-electrode system consisted of a glassy carbon electrode as working electrode, an Ag/AgCl (sat. KCl) as reference electrode, and platinum gauze as counter electrode. All potential values are reported as a function of Ag/AgCl. The surface conductivity (surface resistance) of samples was measured at room temperature by four-point probe method using Advanced Instrument Technology CMT-SR1000N with Jandel Engineering probe. The reported conductivity values are averages of 10 measurements.

Functionalization of MWNT

Into a resin flask equipped with high-torque mechanical stirrer, nitrogen inlet and outlet, 4-aminobenzoic acid (10.0 g, 73 mmol), MWNT (5.0 g), PPA (300.0 g, 83% P_2O_5 assay), and P_2O_5 (75.0 g) were placed. The flask was immersed in oil bath and gently heated to 100 °C. The reaction mixture was stirred at the temperature for 1 h. The reaction mixture was then heated to 130 °C and stirred for 72 h under nitrogen atmosphere. The dark homogeneous mixture was poured into water. The precipitates were collected by suction filtration and Soxhlet extracted with distilled water for 3 days and methanol for 3 days and finally freeze-dried for 48 h to yield 9.82 g (71.7% yield) of dark black powder. Anal. Calcd. for $C_{12.71}H_6O_1N_1$: C, 80.89%; H, 3.21%; N, 7.42%. Found: C, 79.06%; H, 2.20%; N, 5.45%.

Synthesis of PANi Homopolymer

Into a 250-mL, three-necked, round-bottom flask equipped with a magnetic stirring bar, a reflux condenser, and a nitrogen inlet, aniline (10.0 g, 0.107 mol) and 1 M HCl (120 mL) were charged. An 80 mL of 1 M HCl solution containing APS (30.0 g, 0.131 mol) was added dropwise into the solution with constant mechanical stirring at the reaction

temperature range of 0–5 °C for 1 h. The reaction mixture was stirred for additional 6 h at 0–5 °C. The dark green precipitate was collected by suction filtration and washed with distilled water and methanol. The resultant solids were transferred to an extraction thimble and Soxhlet extracted with water for 3 days and methanol for 3 days and finally freeze-dried under reduced pressure for 48 h to yield 5.56 g of dark green PANi powder. Found: C, 65.42%; H, 4.36%; N, 11.51%. As the level of HCl doping was unknown, the yield and theoretical carbon–hydrogen–nitrogen (CHN) contents could not be precisely calculated.

Model Reaction of AF-MWNT with *N,N*-Dimethylaniline

Into the same experimental setup and procedure for the synthesis of PANi homopolymer, AF-MWNT (0.2 g), *N,N*-dimethylaniline (1.8 g, 0.015 mol), and 1 M HCl (10 mL) were charged. A total of 1.0 M HCl solution (10 mL) containing APS (3.0 g, 0.013 mol) was added dropwise into the suspension with constant mechanical stirring in the reaction temperature range of 0–5 °C for 1 h. The reaction mixture was stirred for additional 6 h at 0–5 °C. The black precipitate was collected by suction filtration and washed with distilled water. The resultant solids were transferred to a glass extraction thimble and Soxhlet extracted with water for 3 days and methanol for 3 days. For dedoping, the thimble was immersed into aqueous ammonia (1 M) at room temperature for 24 h and then freeze-dried under reduced pressure for 48 h. Thus, obtained was 0.17 g of black powder as dedoped (4-(4-dimethylamino)phenylamino)benzoyl-functionalized MWNT (DB-MWNT). Anal. Calcd. for $C_{168.65}H_{193.19}N_{19.82}O$: C, 80.58%; H, 7.75%; N, 11.04%. Found: C, 78.01%; H, 2.31%; N, 5.09%.

Grafting of PANi onto AF-MWNT

Into the same experimental setup for the synthesis of PANi homopolymer, AF-MWNT (1.0 g), aniline (9.0 g, 96.6 mmol), and 1 M HCl (120 mL) were charged. An 80 mL of 1.0 M HCl solution containing APS (30.0 g, 0.131 mol) was added dropwise into the suspension. The rest of reaction and workup procedures were the same as the synthesis of PANi homopolymer. The resultant dark purple-colored powder was also freeze-dried under the reduced pressure for 48 h to give 10.54 g of PANi-*g*-MWNT. Found: C, 61.29%; H, 4.57%; N, 10.85%. As the level of HCl doping in PANi was unknown, the yield and theoretical CHN contents could not be precisely calculated.

Dedoping of PANi and PANi-*g*-MWNT

As-prepared partially doped (protonated) PANi and PANi-*g*-MWNT were dedoped (deprotonated) by immersion of the samples into basic 1 M aqueous ammonia at room temperature for 24 h. Dedoped PANi and PANi-*g*-MWNT were collected by suction filtration, washed with deionized water, and finally freeze-dried under reduced pressure for 48 h. PANi: Anal. Calcd. for $C_6H_5N_1$: C, 79.10%; H, 5.53%; N, 15.37%. Found: C, 69.59%; H, 4.39%; N, 13.48%. PANi-*g*-MWCNT: Anal. Calcd. for $C_{164.12}H_{127.65}O_1N_{25.53}$: C, 79.69%; H, 5.21%; N, 14.45%. Found: C, 74.09%; H, 4.55%; N, 13.67%.

Doping of PANi and PANi-*g*-MWNT

The dedoped PANi and PANi-*g*-MWNT samples were doped (protonated) by immersion in 1 M HCl at room temperature for 48 h. The workup procedure was the same as dedoping of PANi and PANi-*g*-MWNT. Found for PANi: C, 62.29%; H, 4.22%; N, 11.80%; Found for PANi-*g*-MWNT: C, 63.60%; H, 4.55%; N, 11.66%. The yield and theoretical CHN contents could not be precisely calculated because the degree of doping was not known.

Blends of AF-MWNTs with PANi

AF-MWNTs (0.01 g) and dedoped PANi (0.09 g) and NMP (10 mL) were placed in a 20-mL vial and were stirred with magnetic stirrer at room temperature. After 24 h, they were precipitated in deionized water. The resultant black powder was freeze-dried for 48 h to afford PANi/MWNT. Some PANi/MWNT samples were doped (protonated) by immersion in 1 M HCl at room temperature for 48 h.

RESULTS AND DISCUSSION

Functionalization of MWNT

As described in the literature procedure,[22] the functionalization of MWNT was carried out with 4-aminobenzoic acid in PPA/P_2O_5 medium at 130 °C [Fig. 1(a)]. The resultant AF-MWNT was decorated by 4-aminobenzoyl moieties, which could be reactive sites to graft PANi via chemical oxidation polymerization. The CHN contents from EA (see Supporting Information for detailed calculation) and approximate theoretical values are summarized in Table 1. There are noticeable difference between theoretical and measured values in the EA, which could be caused by a number of factors, such as the relative hygroscopic nature of these chemically modified carbon nanomaterials. Given that this type of materials is not easily quantified using destructive thermal characterization methods, the results may have overestimated the actual extent of functionalization.

Model Reaction of AF-MWNT with *N,N*-Dimethylaniline and Grafting of PANi onto the Surface of AF-MWNT

The covalent bond formation between AF-MWNT and PANi via chemical oxidation polymerization could be conceivable by the model reaction between AF-MWNT and *N,N*-dimethylaniline [Fig. 1(b)].

To graft PANi onto the surface of AF-MWNT, aniline was treated with AF-MWNT (10 wt %) in APS/1 M HCl at 0–5 °C [Fig. 1(c)]. The resultant composite, PANi-grafted MWNT (PANi-*g*-MWNT), was prepared and it was expected to show improved solution and solid-state processability as well as enhanced conductivity. As the reference material, the PANi homopolymer was prepared in the same reaction condition as described in Figure 1(d).

Solubility

PANi was soluble well in trifluoroacetic acid (CF_3COOH), phenol, tetrahydrofuran (THF), carbon disulfide (CS_2), and polar aprotic solvents such as *N,N*-dimethylformamide (DMF), *N,N*-dimethylacetamide (DMAc), dimethyl sulfoxide (DMSO), and NMP. The solutions of PANi showed various colors such as light yellow, blue, and light green depending

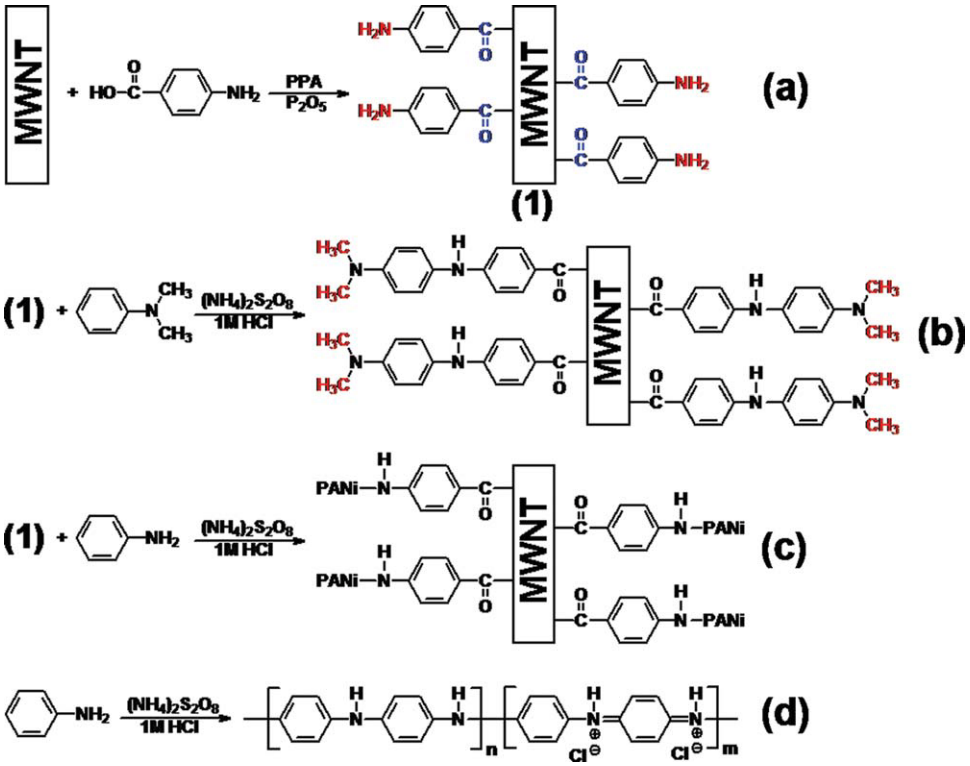

FIGURE 1 (a) Functionalization of MWNT in PPA/P_2O_5, (b) grafting of *N,N*-dimethylaniline onto the surface of AF-MWNT in APS/HCl (1 M), (c) grafting of PANi onto the surface of AF-MWNT in APS/HCl (1 M), and (d) polymerization of aniline in APS/HCl (1 M). The structure for functionalized and PANi-*g*-MWNT is idealized for easy visualization of the concept present here. [Color figure can be viewed in the online issue, which is available at www.interscience.wiley.com.]

upon solvent used. Although the PANi-*g*-MWNT was not completely soluble in all of aforementioned solvents, the solution colors turned to light black in CF_3COOH, light yellow in phenol, and blue in NMP, which indicated that the sample was quite soluble in these solvents.

FTIR Study

To exclude unexpected variables, all samples were thoroughly worked up with a Soxhlet extraction in water for 3 days to remove any residual reaction medium and in methanol for 3 days to get rid of low-molecular-mass impurities such as unreacted *N,N*-dimethylaniline for DB-MWCNT, 4-aminobenzoic acid for AF-MWNT, and aniline for both PANi and PANi-*g*-MWNT.

To verify the covalent attachment of 4-aminobenzoyl moieties, FTIR is a commonly used and powerful tool for this purpose. The existence of $sp^2C—H$ and $sp^3C—H$ stretching bands at 2969 cm^{-1} attributable to the defects at sidewalls and open ends of MWNT was previously reported.[23] The

TABLE 1 Elemental Analysis of Samples

Sample	Condition	EF	FW (g mol^{-1})		C (%)	H (%)	N (%)
AF-MWNT	As-prepared	$C_{12.71}H_6NO$	188.76	Calcd.	80.89	3.21	7.42
				Found	79.06	2.20	5.45
DB-MWNT	As-prepared	NA	NA	Found	78.01	2.31	5.09
	Dedoped	$C_{168.65}H_{193.19}N_{19.82}O$	2514.0	Calcd.	80.58	7.75	11.04
				Found	78.01	2.31	5.09
	Doped	NA	NA	Found	79.00	2.29	5.04
PANi	As-prepared	NA	NA	Found	65.42	4.36	11.51
	Dedoped	C_6H_5N	91.11	Calcd.	79.10	5.53	15.37
				Found	69.59	4.39	13.48
	Doped	NA	NA	Found	62.29	4.22	11.80
PANi-*g*-MWNT	As-prepared	NA	NA	Found	61.29	4.57	10.85
	Dedoped	$C_{164.12}H_{127.65}N_{25.53}O$	2473.5	Calcd.	79.69	5.21	14.45
				Found	74.09	4.55	13.67
	Doped	NA	NA	Found	63.60	4.55	11.66

EF, empirical formula; FW, formula weight; NA, not applicable.

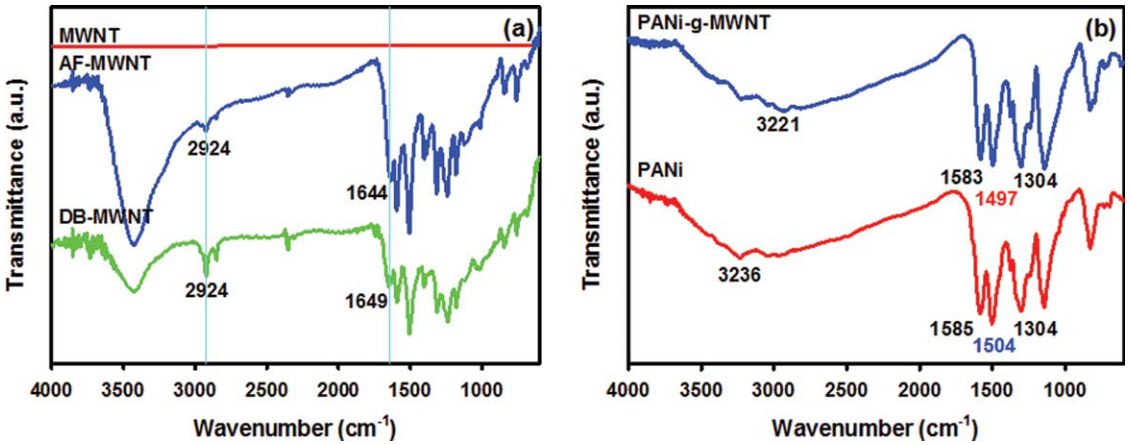

FIGURE 2 FTIR (KBr pellet) spectra: (a) MWNT, AF-MWNT, and DB-MWNT and (b) PANi and PANi-*g*-MWNT. [Color figure can be viewed in the online issue, which is available at www.interscience.wiley.com.]

defects, which were primarily responsible for the "direct" Friedel-Crafts acylation, are originated during the synthesis of MWNT from hydrocarbon feedstock.[20] However, some complex and destructive addition reaction could not be excluded for the effective functionalization of CNT, because a model study on defect-free fullerene (C_{60}) under the same reaction conditions has demonstrated that such regioselective, destructive addition reaction leading to Friedel-Crafts acylation products could occur.[24]

The FTIR spectrum [Fig. 2(b)] obtained from the resultant model compound (DB-MWNT) shows a much stronger sp^3C—H peak at 2924 cm^{-1} compared to that of AF-MWNT [Fig. 2(a)]. The aromatic keto-carbonyl (C=O) peak at 1644 cm^{-1} confirmed that MWNTs were successfully functionalized with 4-aminobenzoyl moieties to yield AF-MWNT.

The PANi homopolymer displayed the characteristic bands of secondary amine (N—H) at 3226 cm^{-1}, the C=C stretching deformation of the quinoid at 1585 cm^{-1}, benzenoid rings at 1504 cm^{-1}, and the C—N stretching of the secondary aromatic amine at 1304 cm^{-1} [Fig. 2(b)]. The PANi-*g*-MWNT displayed almost identical characteristic bands at 3231, 1583, 1497, and 1304 cm^{-1}. Compared to the number of PANi repeating units in PANi-*g*-MWNT composite, the relative population of C=O groups was too low to be clearly detected, because they were only located at the covalent junction between AF-MWNT and PANi.

Wide-Angle X-Ray Diffraction

To determine the morphologies of AF-MWNT, PANi, and PANi-*g*-MWNT, as-prepared powder samples after Soxhlet extraction were subjected to WAXD scans. The AF-MWNT displayed *d*-spacing values at 2.10 ($2\theta = 43.12°$), 3.47 ($2\theta = 25.65°$), and 4.33 Å ($2\theta = 20.48°$). The peak at 3.47 Å corresponds to wall-to-wall distance of MWNT [Fig. 3(a)]. The PANi showed a broad amorphous peak with relatively weaker crystalline peaks at $2\theta = 19.74°$ and 25.52° [Fig. 3(b)]. It was an indication that major portion of PANi homopolymer was comprised of an amorphous phase. It has been reported that the dedoped PANi in base form exhibited different structural characteristics.[25] Its diffraction patterns show semicrystalline nature with one very distinct Bragg's peak at $2\theta \approx 19°$ and two less intense peaks at $2\theta \approx 24°$ and 31°.[25] That means the dopant should affect the crystal structure and crystallinity of PANi. It has also been reported that the crystallinity of PANi is increased after doping with HCl.[26] Therefore, although it could not be completely removed, lower crystallinity of PANi in this study implied that the significant amount of bound HCl during the polymerization was removed during Soxhlet extraction for several days with distilled water and methanol (see Experimental section).

The PANi-*g*-MWNT displayed three peaks at $2\theta = 14.59°$, 20.17°, and 24.97°. This means that crystallinity was present even after most of HCl dopant had been removed during the course of Soxhlet extraction. The much higher crystallinity of PANi-*g*-MWNT than that of PANi could be due to MWNT, which could act as nucleation sites for PANi. The new peak

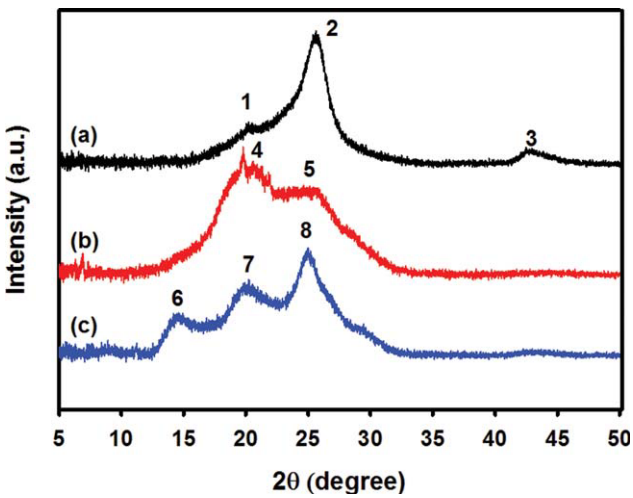

FIGURE 3 WAXD patterns: (a) AF-MWNT, (b) PANi, and (c) PANi-*g*-MWNT. [Color figure can be viewed in the online issue, which is available at www.interscience.wiley.com.]

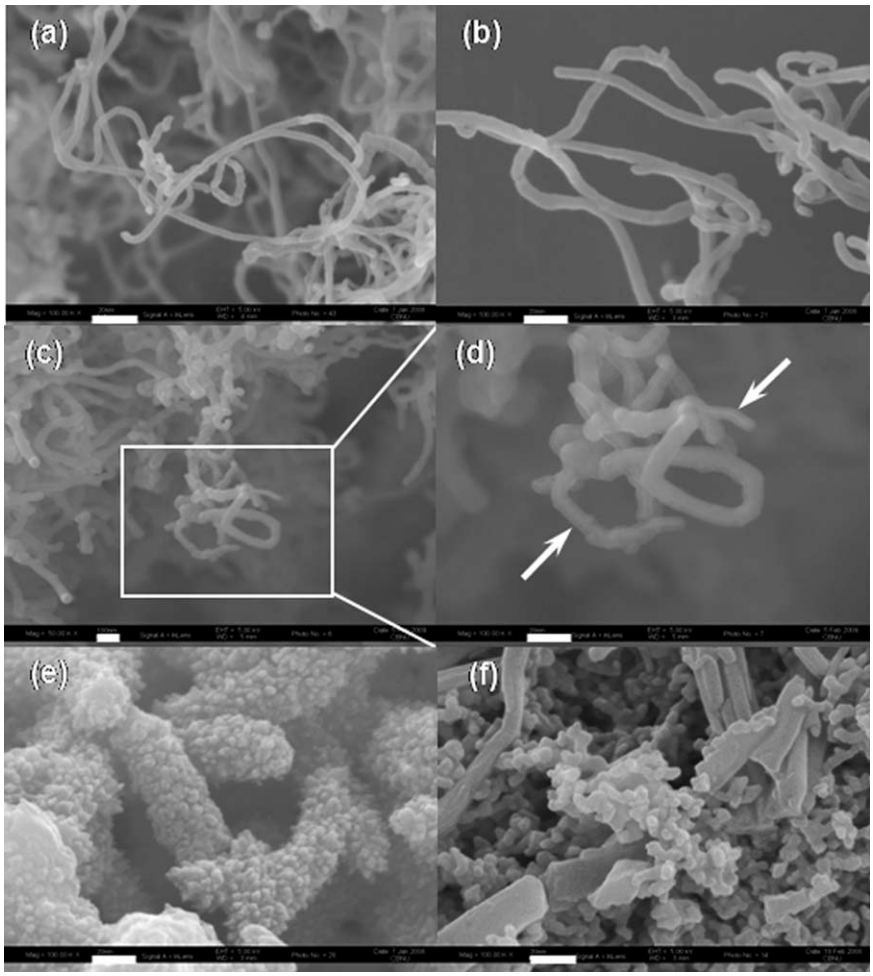

FIGURE 4 SEM images: (a) as-received MWNT (100,000×), (b) AF-MWNT (100,000×), (c) DB-MWNT (50,000×), (d) DB-MWNT (100,000×), (e) PANi-*g*-MWNT (100,000×), and (f) PANi (100,000×). Scale bars are 100 nm.

at 14.59° [Fig. 3(c)] is related epitaxial crystal growth onto AF-MWNT. The relatively poor solubility of PANi-*g*-MWNT could also contribute to a result of the higher crystallinity of PANi in it.

Scanning Electron Microscopy

In comparing the SEM results depicted in Figure 4, the SEM image of pristine MWNT shows that the tubes have relatively seamless and smooth surfaces [Fig. 4(a)] before chemical modification. The average diameter of pristine MWNT is 10–20 nm. The diameters of AF-MWNT, DB-MWNT, and PANi-*g*-MWNT are clearly larger than that of pristine MWNT, most probably because of covalently anchored chemical moieties and some small-scale bundling (Fig. 4). The average diameter of AF-MWNT is ∼40 nm, which is much larger than pristine MWNT (10–20 nm) [Fig. 4(b)]. As the relatively smaller size of 4-aminobenzoyl (∼0.7 nm, based on molecular mechanics modeling) does not account for the apparently large increase in the diameter (∼20–30 nm) of AF-MWNT, we suspect that the polar nature of 4-aminobenzoyl pendants might, which could form much stronger lateral interaction along AF-MWNT, have encouraged the formation of small bundles of AF-MWNT comprising four to seven individual AF-MWNT tubes.[22(c)] In the case of DB-MWNT, the average diameter is about 50 nm [Fig. 4(c)]. The core-shell structure of DB-MWNT was observable in high-magnification SEM images [Fig. 4(d), arrows]. The inner hard core was noted to be of the order of 10–20 nm, which is closer to the diameter of pristine MWNT. The outer soft shell structure is most likely due to the (4-(4-dimethylamino)phenylamino)benzoyl moiety that has uniformly covered the surface of AF-MWNT. The average diameter of PANi-*g*-MWNT is ∼200 nm, which is much larger than pristine MWNT as well as AF-MWNT. These results agree with the notion that PANi has been grafted onto the surface of AF-MWNT. In addition, the surface of PANi-*g*-MWNT is covered with many protrusions, which must be PANi crystals [Fig. 4(e)]. In the case of PANi homopolymer, nanosized rods and irregular particles coexisted because of rigid-rod nature of PANi chains and secondary growth of PANi [Fig. 4(f)].[27] As PANi-*g*-MWNT did not show any irregularly formed, independent particles, it is postulated that AF-MWNT nucleation must have prevented the generation of these irregular PANi particles. The overall SEM results further support that PANi has been covalently grafted onto the surface of AF-MWNT.

To compare with PANi-*g*-MWNT, the AF-MWNT blended with PANi (PANi/MWNT) was prepared by physical blend of PANi and AF-MWNT in NMP. The SEM images obtained from PANi/MWNT (Fig. 5) show the clear difference from PANi-*g*-

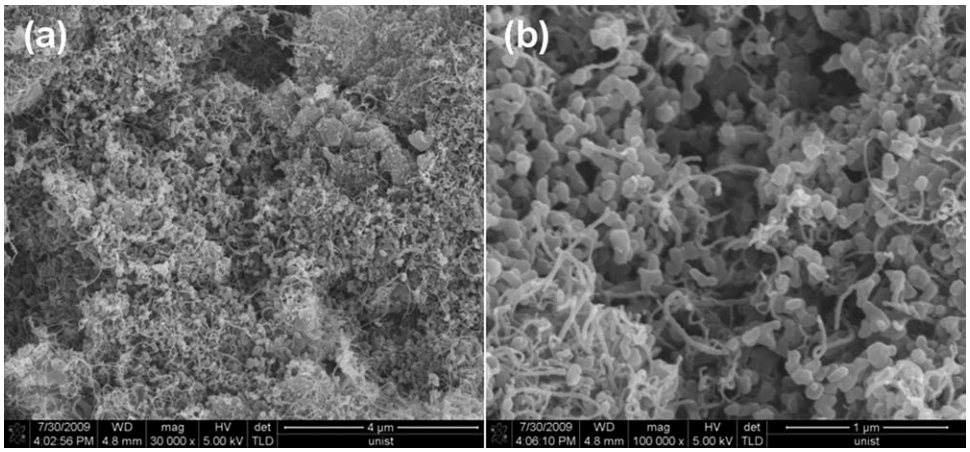

FIGURE 5 SEM images of PANi/MWNT blend system: (a) 30,000× and (b) 100,000×.

MWNT [Fig. 4(e)]. Although the PANi/MWNT blend system shows that AF-MWNT is dispersed well into PANi matrix, the average diameter of PANi/MWNT is much smaller at 40 nm, which is close to that of AF-MWNT [Fig. 5(a,b)]. The result supported that AF-MWNT in the blend system did not serve as nucleation agent to PANi. In turn, the result implied that AF-MWNT in PANi-*g*-MWNT indeed provided its surface as nucleation sites.

Transmission Electron Microscopy

To further assure that MWNT remained intact during the reaction and workup sequence and also to verify the covalent attachment of PANi onto the surface of MWNT, TEM study was conducted. For the TEM sample, PANi-*g*-MWNT was dispersed in NMP; a carbon-coated copper grid was dipped into this mixture and taken out to dry in a vacuum oven. The TEM images of PANi-*g*-MWNT show that the AF-MWNT was heavily decorated with PANi [Fig. 6(a)]. Furthermore, the distinct graphitic planes from the MWNT framework at higher magnification implicate that MWNT was not damaged during the grafting polymerization reactions and workup process [Fig. 6(b)]. The unique microscopic results from SEM and TEM explained that the two reaction conditions applied in this work are indeed effective for the functionalization and grafting of MWNT. Hence, it could be concluded that PANi was efficiently grafted onto the surface of the AF-MWNT to afford PANi-*g*-MWNT composite.

BET Surface Area

For the BET surface measurements, the PANi and PANi-*g*-MWNT were dedoped to minimize the effect of dopants. The powder samples were degassed under vacuum at 100 °C before measurement. The BET surface areas of PANi and PANi-*g*-MWNT were 65 and 52 $m^2\ g^{-1}$, respectively, (Table 2). The surface area of PANi-*g*-MWNT was almost 19% lower than PANi. This could be due to a more compact morphology of PANi-*g*-MWNT, which also showed higher crystallinity. Both WAXD and SEM results [see Figs. 3 and 4(e), respectively] support that AF-MWNT served as both grafting and nucleating sites for PANi, which covalently linked and crystallized on AF-MWNT surface. The uniform grafting and nucleation also suppressed the formation of irregular PANi particles.

Thermooxidative Stability

The thermooxidative stability of different powder samples in air was studied using TGA. The weight loss of AF-MWNT was ∼49% around 660 °C, where the two curves of pristine MWNT and AF-MWNT intersected (Fig. 7). It strongly implied that tremendous amount of 4-aminobenzoyl moieties was covalently attached to the surface of AF-MWNT. In the cases of PANi and PANi-*g*-MWNT, to eliminate the effect of volatile HCl at elevated temperature, both samples were converted into the base form by immersing them into 1 M aqueous ammonia solution and dried before they were subject to TGA measurement. As shown in Figure 7, the PANi and PANi-*g*-MWNT displayed that the temperature at which 5% weight loss ($T_{d5\%}$) in air occurred at 258 and 333 °C, respectively. The char yields of those in air at 800 °C were almost 0% for both samples. The thermooxidative stability of PANi-*g*-MWNT was ∼75 °C higher than that of PANi homopolymer.

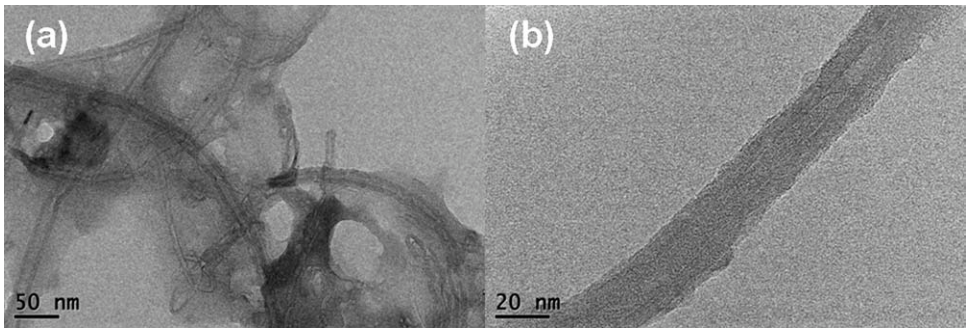

FIGURE 6 TEM images of PANi-*g*-MWNT: (a) 50,000× and (b) 150,000×.

TABLE 2 BET Surface Area, Pore Volume, and Average Pore Size of PANi and PANi-*g*-MWNT

Sample	Surface Area ($m^2\ g^{-1}$)	Pore Volume ($mL\ g^{-1}$)	Pore Size (Å)
Dedoped PANi	64.6	0.00381	144
Dedoped PANi-*g*-MWNT	52.3	0.01011	200

UV–Vis Absorption and Emission Behaviors

UV–vis absorption and emission measurements were conducted to study the interfacial interaction between PANi and MWNT. Stock solution (10 mg L^{-1}) of each sample was prepared in NMP. The UV absorption of PANi showed two peaks at 317 and 618 nm. Both peaks are related to the $\pi \rightarrow \pi^*$ transition of benzenoid ring and quinoid ring in PANi, respectively, which are identical to those of dedoped PANi.[28] These results agree with WAXD results that most of HCl was removed (dedoped) from both PANi and PANi-*g*-MWNT during Soxhlet extraction. Compared to the PANi homopolymer, which showed peak maxima at 317 and 618 nm, the peaks from PANi-*g*-MWNT red-shifted by 6 and 11 nm and showed maxima at 323 and 629 nm, respectively [Fig. 8(a)]. This implies that there is a strong interaction between PANi and MWNT, and PANi is covalently grafted onto the surface of AF-MWNT.

Fluorescent measurements of the samples were conducted using the applied excitation wavelength corresponding to UV absorption maximum of each sample. The emission maxima of PANi and PANi-*g*-MWNT were at 402 and 404 nm, respectively [Fig. 8(b)]. Both peaks were almost identical, which could be due to the fact that PANi was uniformly grafted onto the surface of AF-MWNT. A uniform covalent coating of PANi suppressed the MWNT influence at excited state. If MWNT and PANi were physically aggregated by intermolecular π–π interaction in solid state and were segregated in solution, the emission intensity of PANi-*g*-MWNT would be much weaker or the peak location should be significantly shifted. This is due to the fact that CNTs can act as strong excimer quenchers and light absorbers.[29]

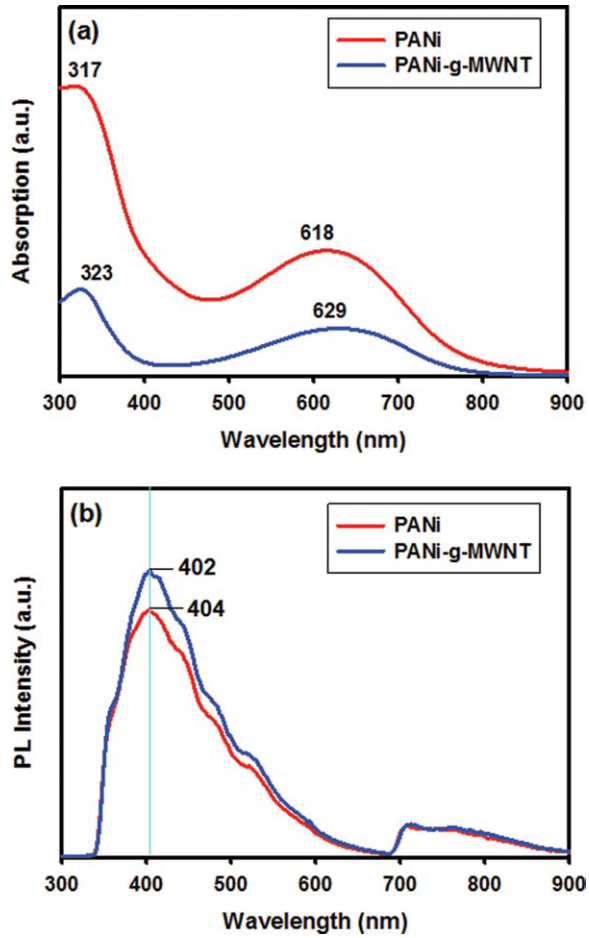

FIGURE 8 UV–vis absorption and emission spectra of PANi and PANi-*g*-MWNT: (a) absorption and (b) emission.

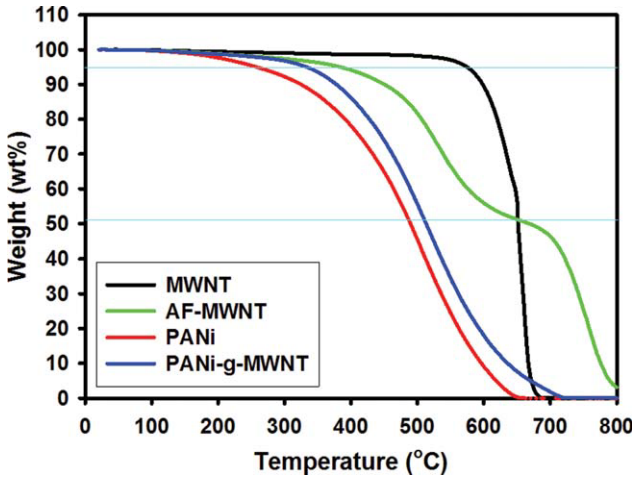

FIGURE 7 TGA thermograms of samples in air with a heating rate of 10 °C min^{-1}.

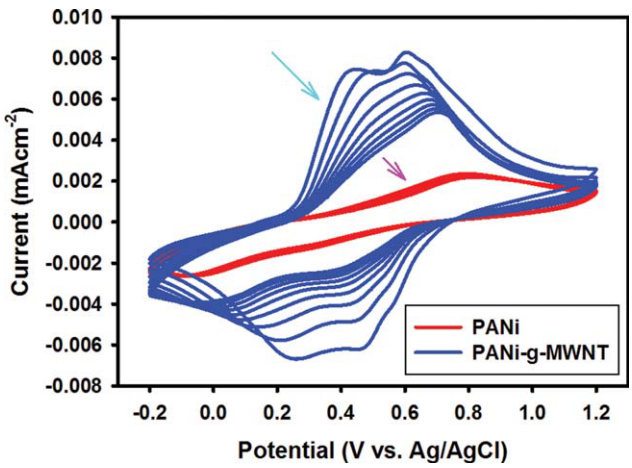

FIGURE 9 Cyclic voltammograms of PANi and PANi-*g*-MWNT in 1.0 M H_2SO_4 aqueous solution. Scan rate is 10 mV s^{-1}.

TABLE 3 Conductivities of PANi, PANi-*g*-MWNT, and PANi/MWNT with Respect to Their Doping State

State	Sample	Conductivity (S cm^{-1})
After Soxhlet extraction	PANi	2.09×10^{-6}
	PANi-*g*-MWNT	1.88×10^{-3}
Dedoped with 1 M NH_3 (aq.)	PANi	Out of measuring limit
	PANi-*g*-MWNT	Out of measuring limit
Doped with 1 M HCl	PANi	1.09×10^{-2}
	PANi-*g*-MWNT	1.01×10^{-1}

Cyclic Voltammetry

CV has generally been used to investigate the electrochemical properties of conductive materials. PANi and PANi-*g*-MWNT were characterized by CV using a three-electrode electrochemical cell. During the first scan of PANi, the broad oxidation and reduction (redox) peaks were observed at about 0.78 and −0.06 V versus Ag/AgCl, respectively (Fig. 9). These values are related to the redox of the PANi from emeraldine state to pernigraniline state.[30] The output current of PANi-*g*-MWNT was observed to be much larger that of pure PANi. The PANi-*g*-MWNT displayed well-behaved redox process from the first to ninth scan (see arrows). The capacitance was estimated from the output current divided by the scan rate. The specific capacitance of PANi-*g*-MWNT was found to be much larger than that of pure PANi. Although the surface area of PANi-*g*-MWNT was smaller than that of pure PANi homopolymer (see Table 2), the improvement in specific capacitance can be attributed to the good conductivity of MWNT. The results suggest that ion inclusion and exclusion in PANi-*g*-MWNT were much more effective during the redox process.

Electrical Conductivity

All test specimens were prepared by compression molding at high pressure (60 MPa). The conductivity at room temperature was measured at 10 different locations and averaged. The values were determined using the following equation $\sigma = 1/(\rho^{*}\mathrm{cf}^{*}d)$, where σ, ρ, cf, and d are the conductivity, the resistivity, the correction factor (4.340), and the sample thickness, respectively.[31] The conductivity of as-prepared PANi-*g*-MWNT after Soxhlet extraction was 1.88×10^{-3} S cm^{-1}. This is ~900 times higher than the value obtained from as-prepared PANi homopolymer (Table 3). Both values indicate that a trace amount of HCl may still remain in the matrices and play as a dopant. However, WAXD and UV results have indicated that HCl was almost completely removed during Soxhlet extraction. After measuring the conductivities of as-prepared PANi and PANi-*g*-MWNT, the samples were converted into the base form by treatment with 1 M aqueous ammonia. The conductivities of dedoped PANi and PANi-*g*-MWNT were out of detection limit (1×10^{-6} S cm^{-1}). These results further implicate the existence of residual dopants because the conductivity of dedoped PANi is generally in the range of 10^{-5} to 5×10^{-6} S cm^{-1}. The dedoped PANi and PANi-*g*-MWNT were doped by immersion into 1 M aqueous HCl solution and dried. The redoped PANi-*g*-MWNT displayed a good conductivity of 1.01×10^{-1} S cm^{-1}, which was in the semimetallic region. This value was ~10 times higher than the conductivity of redoped PANi (1.09×10^{-2} S cm^{-1}). Thus, the conductivity of PANi was significantly improved by grafting onto the surface of MWNT. This is due to the fact that the charge transfer from electron-rich PANi to electron-deficient MWNT is quite efficient.[3,32] Similar result was recently reported by Lee and coworkers that an *in situ* nanocomposite containing 10 wt % CO_2H-functionalized MWNT and PANi doped with dodecyl sulfate and prepared via an emulsion polymerization of aniline showed an electrical conductivity of 2.72×10^{-1} S cm^{-1}.[33]

CONCLUSIONS

The MWNT was first functionalized with 4-aminobenzoic acid to afford AF-MWNT, which was subsequently grafted with PANi via an *in situ* polymerization to generate a PANi-*g*-MWNT nanocomposite. The resultant materials (AF-MWNT, PANi, and PANi-*g*-MWNT) were studied with various analytical techniques such as FTIR, WAXD, SEM, TEM, TGA, UV–vis, and fluorescence spectroscopy. From the CV and conductivity measurements, PANi-*g*-MWNT displayed significantly improved conductivity and capacitance over PANi homopolymer. Thus, we demonstrated that the two-step reaction sequence for the Friedel-Crafts functionalization of MWNT and the subsequent grafting of PANi onto the surface of AF-MWNT are indeed a feasible approach to hybridization of carbon-based nanomaterials and functional polymers. Our approach could be viewed as a comparable route to the *in situ* emulsion polymerization of aniline in the presence of carboxylic acid–functionalized MWNT recently reported by Lee and coworkers.[33] As a result, it is a reasonable expectation that synergistic enhancement could be obtained from the special attributes of each component, leading to the development of a new class of advanced materials for various electronic and optoelectronic applications. And also, we supposed that if new hybridized materials, which are made by Friedel-Crafts functionalization and grafting of polymers with CNT as conductive dopants, will display better conductivity.

The authors are grateful to Jeong Hee Lee of Chungbuk National University for conducting SEM. This project was supported by funding from US Air Force Office of Scientific Research, Asian Office of Aerospace R and D (AFOSR-AOARD) and National Research Foundation (D00267).

REFERENCES AND NOTES

1 (a) Tasis, D.; Tagmatarchis, N.; Bianco, A.; Prato, M. Chem Rev 2006, 106, 1105–1136; (b) Grossiord, N.; Loos, J.; Regev, O.; Koning, C. E. Chem Mater 2006, 18, 1089–1099; Balasubramanian, K.; Burghard, M. Small 2005, 1, 180–192; (d) Banerjee, S.; Kahn, M. G. C.; Wong, S. S. Chem Eur J 2003, 9, 1898–1908.

2 (a) Pradhan, B.; Setyowati, K.; Liu, H.; Waldeck, D. H.; Chen, J. Nano Lett 2008, 8, 1142–1146; (b) Wang, F.; Gu, H.; Swager, T. M. J Am Chem Soc 2008, 130, 5392–5393; Wei, C.; Dai, L.; Roy, A.; Tolle, T. B. J Am Chem Soc 2006, 128, 1412–14132 (d) Wu, T. M.; Lin, Y. W. Polymer 2006, 47, 3576–3582.

3 Zengin, H.; Zhou, W.; Jin, J.; Czerw, R.; Smith, D. W., Jr.; Echegoyen, L.; Carroll, D. L.; Foulger, S. H.; Ballato, J. Adv Mater 2002, 14, 1480–1483.

4 Woo, H. S.; Czerw, R.; Webster, S.; Carroll, D. L.; Park, J. W.; Lee, J. H. Synth Met 2001, 116, 369–372.

5 Kymakis, E.; Amaratunga, G. A. J. J Appl Phys Lett 2002, 80, 112–114.

6 Ago, H.; Petritsch, K.; Shaffer, M. S. P.; Windle, A. H.; Friend, R. H. Adv Mater 1999, 11, 1281–1285.

7 Cheng, G.; Zhao, J.; Tu, Y.; He, P.; Fang, Y. Anal Chim Acta 2005, 533, 11–16.

8 Qu, F.; Yang, M.; Jiang, J.; Shen, G.; Yu, R. Anal Biochem 2005, 344, 108–114.

9 An, K. H.; Jeong, S. Y.; Hwang, H. R.; Lee, Y. H. Adv Mater 2004, 16, 1005–1009.

10 Lefenfeld, M.; Blanchet, G.; Rogers, J. A. Adv Mater 2003, 15, 1188–1191.

11 Huang, W.; Humphrey, B. D.; MacDiarmid, A. G. J Chem Soc Faraday Trans 1986, 82, 2385–2400.

12 (a) Argun, A. A.; Aubert, P. H.; Thompson, B. C.; Schwendeman, I.; Gaupp, C. L.; Hwang, J.; Pinto, N. J.; Tanner, D. B.; MacDiarmid, A. G.; Reynolds, J. R. Chem Mater 2004, 16, 4401–4412; (b) Kugler, T.; Lögdlund, M.; Salaneck, W. R. Acc Chem Res 1999, 32, 225–234.

13 Nicolas-Debarnot, D.; Poncin-Epaillard, F. Anal Chim Acta 2003, 475, 1–15.

14 Huang, S. C.; Ball, I. J.; Kaner, R. B. Macromolecules 1998, 31, 5456–5464.

15 Trivedi, D. C.; Dhawan, S. K. J Mater Chem 1992, 2, 1091–1096.

16 (a) Ali, S. R.; Ma, Y.; Parajuli, R. R.; Balogun, Y.; Lai, W. Y. C.; He, H. Anal Chem 2007, 79, 2583–2587; (b) Guo, L.; Peng, Z. Langmuir 2008, 24, 8971–8975; (c) Liu, J.; Tian, S.; Knoll, W. Langmuir 2005, 21, 5596–5599; (d) Panhuis, M. I. H.; Doherty, K. J.; Sainz, R.; Benito, A. M.; Maser, W. K. J Phys Chem C 2008, 112, 1441–1445; (e) Sainz, R.; Small, W. R.; Young, N. A.; Vallés, C.; Benito, A. M.; Maser, W. K.; Panhuis, M. I. H. Macromolecules 2006, 39, 7324–7332; (f) Yan, X. B.; Han, Z. J.; Yang, Y.; Tay, B. K. J Phys Chem C 2007, 111, 4125–4131.

17 (a) Chen, J.; Rao, A. M.; Lyuksyutov, S.; Itkis, M. E.; Hamon, M. A.; Hu, H.; Cohn, R. W.; Eklund, P. C.; Colbert, D. T.; Smalley, R. E.; Haddon, R. C. J Phys Chem B 2001, 105, 2525–2528; (b) Ramesh, S.; Ericson, L. M.; Davis, V. A.; Saini, R. K.; Kittrell, C.; Pasquali, M.; Billups, W. E.; Adams, W. W.; Hauge, R. H.; Smalley, R. E. J Phys Chem B 2004, 108, 8794–8798.

18 (a) Monthioux, M.; Smith, B. W.; Burteaux, B.; Claye, A.; Fischer, J. E.; Luzzi, D. E. Carbon 2001, 39, 1251–1272; (b) Salzmann, C. G.; Llewellyn, S. A.; Tobias, G.; Ward, M. A. H.; Huh, Y.; Green, M. L. H. Adv Mater 2007, 19, 883–887; (c) Zhang, Y.; Shi, Z.; Gu, Z.; Iijima, S. Carbon 2000, 38, 2055–2059.

19 Sammalkorpi, M.; Krasheninnikov, A.; Kuronen, A.; Nordlund, K.; Kaski, K. Phys Rev B 2004, 70, 1–8.

20 (a) Baek, J. B.; Lyons, C. B.; Tan, L. S. J Mater Chem 2004, 14, 2052–2056; (b) Jeong, J. Y.; Lee, H. J.; Kang, S. W.; Tan, L. S.; Baek, J. B. J Polym Sci Part A: Polym Chem 2008, 46, 6041–6050; (c) Jeon, I. Y.; Tan, L. S.; Baek, J. B. J Polym Sci Part A: Polym Chem 2008, 46, 3471–3481.

21 Jeon, I. Y.; Lee, H. J.; Choi, Y. S.; Tan, L. S.; Baek, J. B. Macromolecules 2008, 41, 7423–7432.

22 (a) Baek, J. B.; Tan, L. S. Polymer 2003, 44, 4135–4147; Han, S. W.; Oh, S. J.; Tan, L. S.; Baek, J. B. Carbon 2008, 46, 1841–1849; (c) Lee, H. J.; Han, S. W.; Kwon, Y. D.; Tan, L. S.; Baek, J. B. Carbon 2008, 46, 1850–1859.

23 Lee, H. J.; Oh, S. J.; Choi, J. Y.; Kim, J. W.; Han, J.; Tan, L. S.; Baek, J. B. Chem Mater 2005, 17, 5057–5064.

24 Lim, D. H.; Lyons, C. B.; Tan, L. S.; Baek, J. B. J Phys Chem C 2008, 112, 12188–12194.

25 Łuzny, W.; Śniechowski, M.; Laska, J. Synth Met 2002, 126, 27–35.

26 Chen, S. A.; Lee, H. T. Macromolecules 1993, 26, 3254–3261.

27 Huang, J.; Kaner, R. B. J Am Chem Soc 2004, 126, 851–855.

28 Li, G.; Jiang, L.; Peng, H. Macromolecules 2007, 40, 7890–7894.

29 Feng, W.; Fujii, A.; Ozaki, M.; Yoshino, K. Carbon 2005, 43, 2501–2507.

30 (a) Guo, M.; Chen, J.; Li, J.; Tao, B.; Yao, S. Anal Chim Acta 2005, 532, 71–77; (b) Trung, T.; Trung, T. H.; Ha, C. S. Electrochim Acta 2005, 51, 984–990.

31 Perloff, D. S. Solid State Electron 1977, 20, 681–687.

32 Wu, T. M.; Lin, Y. W.; Liao, C. S. Carbon 2005, 43, 734–740.

33 Jeevananda, T.; Siddaramaiah, K.; Kim, N. H.; Heo, S. B.; Lee, J. H. Polym Adv Technol 2008, 19, 1754–1762.